Environ Earth Sci (2016) 75:458
DOI 10.1007/s12665-016-5300-7

ORIGINAL ARTICLE

Protection of neighbour buildings due to construction of shield tunnel in mixed ground with sand over weathered granite

Qing-Long Cui[1] · Huai-Na Wu[2] · Shui-Long Shen[1] · Zhen-Yu Yin[1] · Suksun Horpibulsuk[3]

Received: 23 June 2015 / Accepted: 19 November 2015 / Published online: 10 March 2016

Abstract In south China, many geological formations are composed of weathered rock covered by a thin layer of Quaternary soft deposits, e.g., clayey soil or sandy soil. When the tunnel was constructed in these kinds of compound strata, geohazards such as sinkhole and large settlement are ready to happen. This paper presents a field case of shield tunnelling, which was conducted at the interface of mixed ground between completely weathered granite covered by residual sandy soil at Humen, Guangdong, China. To prevent damage to existing buildings, optimisation of tunnel construction parameters was adopted. During construction, lateral displacements of the subsoil around the tunnel, and horizontal and vertical displacement hazards of seven buildings were monitored. The monitoring results show that maximum settlements and lateral displacements of the buildings were 18.9 and 8.8 mm, respectively, which are all within the allowable value for buildings. The construction parameters such as total thrust, chamber container pressure, grouting pressure and grouting volume are presented and inducing hazards limits to buildings are discussed. The results show that the optimised tunnel construction parameters are sufficient in reducing the hazards of both existing buildings and surrounding soil during tunnel excavation.

Keywords Shield tunnelling · Weathered granite · Hazards

✉ Huai-Na Wu
wu-hn@sjtu.edu.cn

✉ Shui-Long Shen
slshen@sjtu.edu.cn

Qing-Long Cui
cql@sjtu.edu.cn

Zhen-Yu Yin
zhenyu.yin@gmail.com

Suksun Horpibulsuk
suksun@g.sut.ac.th

[1] State Key Laboratory of Ocean Engineering, Department of Civil Engineering, Shanghai Jiao Tong University, Shanghai 200240, China

[2] Department of Civil Engineering, Shanghai Jiao Tong University, Shanghai 200240, China

[3] School of Civil Engineering, Suranaree University of Technology, Nakhon Ratchasima, Thailand

Introduction

Any underground construction process and the use of underground utilities will cause interactions with surrounding ground and may cause hazards to existing facilities. These hazards include injection of hazardous materials (Du et al. 2012, 2014) and ground movements (Xu et al. 2012a; Wu et al. 2014, 2015a; Shen et al. 2015a, b). The underground construction process generally involves temporary works, e.g., deep excavation (Tan and Wang 2013a, b; Cui et al. 2015a, 2016), tunnelling excavation (Liao et al. 2009; Shen et al. 2009, 2010; Cui et al. 2015b), installation of deep mixing columns (Shen et al. 2003) and jet-grouting columns (Wang et al. 2013; Shen et al. 2013a, b), and pile installation. The use of underground utilities may cause long-term deformation due to both loading and geological movement, e.g., the extraction or leakage of groundwater (Xu et al. 2012a, b, 2013a, b, 2014, 2015; Shen et al. 2006, 2014, 2015a, b; Ma et al. 2014; Wu et al. 2014, 2015b, c, d).

Recently in China, with the process of rapid urbanisation, large numbers of underground structures have been

constructed in various types of ground conditions. Railway and metro tunnels make up the largest proportion of underground construction currently in China. As metro railways are usually constructed among crowded urban buildings and structures, it is necessary to investigate the tunnelling excavation effects on adjacent buildings, and hazards prevention methods should be proposed (Liao et al. 2009; Du et al. 2012, 2014).

Many literatures on the physical and mechanical properties have been reported (Dearman 1974, 1978; BSI 1981; Norbury et al. 1995; Ehlen 2002). The granite rock is of high uniaxial compressive strength, which caused the granite or weathered granite to be difficult to break. When constructing the metro tunnels by shield tunnelling method, this kind of weathered granite will appear in front of the excavation face. A number of mixed-ground tunnelling excavations have been reported (Zhao et al. 1994; Shirlaw et al. 2000; Hassanpour et al. 2009; Delisio et al. 2013; Fargnoli et al. 2013). Zhao et al. (2007) described the mixed ground phenomenon and the difficulties encountered when tunnelling through mixed ground in Singapore. Tóth et al. (2013) presented a classification system categorising mixed-face ground and proposed a method to maintain safety in construction and to protect the surrounding ground. Numerical simulations have been used to investigate the interaction between tunnelling excavations and adjacent structures (Addenbrooke and Potts 2001). A new strategy was proposed to predict ground movements and potential damage to the adjacent structures (Shin et al. 2006). Blindheim et al. (2002) studied the effect of mixed face conditions on hard rock Tunnel Boring Machine performance and proposed a protection method for face stability. However, there are very few published field investigation cases recording the impact on adjacent buildings in an "upper-soft and lower-hard" ground, which consists of the soft residual soils formed in Quaternary in the upper layer and the hard weathered granite in the lower layer.

The objective of this paper is to investigate hazards on adjacent buildings during tunnel excavation in completely weathered granite overburdened by residual sandy soil. The interaction between the seven adjacent buildings and the construction procedure is also analysed via field monitoring both of the behaviour of the buildings and the construction parameters.

Project and geology

The Sui-Guan-Shen interurban railway (SGSIR) was a high speed railway linking Guangzhou, Dongguan, and Shenzhen located in Guangdong province, China (Fig. 1a, b). The SGSIR was 74.885 km long and included 14 stations. Taiping Tunnel (14.490 km) and Airport Tunnel (7.816 km) were two of the tunnels of the SGSIR, and were constructed by the shield tunnelling method. Three earth pressure balance shield boring machines (EPBM) were used to excavate Taiping tunnel, which included three stations and two tunnel sections. The test site was located at the south side of Humen Bridge, which was one section of the Taiping Tunnel running from Humen station to Changanxiabian station, measuring 2.893 km in length.

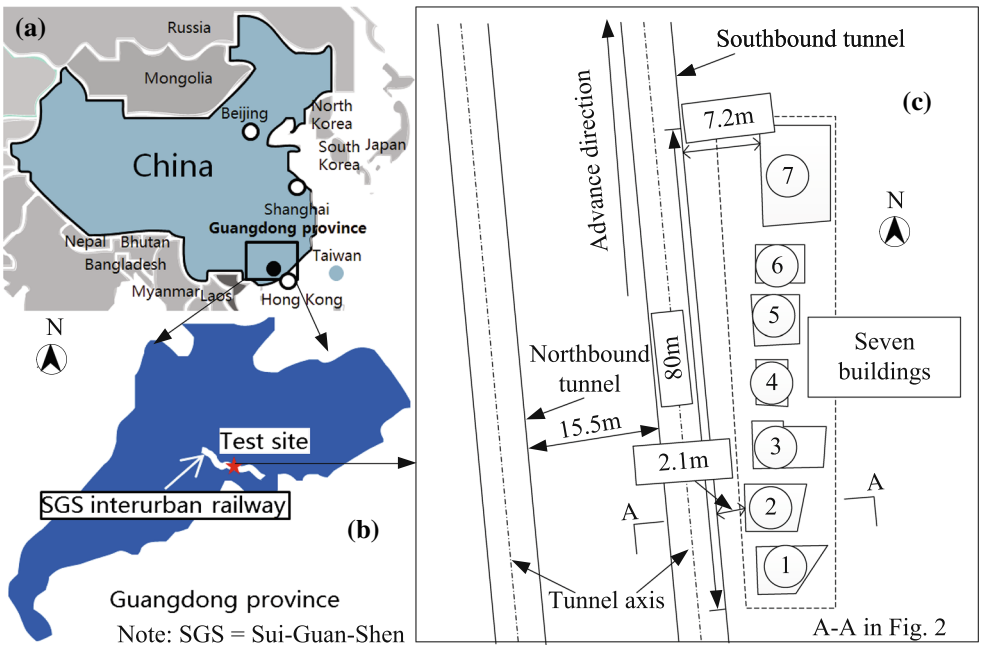

Fig. 1 Location of test site: **a** map of China, **b** location of SGS interurban railway and the test site; **c** plan view of the tunnel and seven buildings

Table 1 General profile of the seven buildings

Building number	Description	Stories	Land area (m^3)	Foundation	Distance from the tunnel (m)	Distance from building 7 (m)
7	Residential building	5	85	Prestressed pipe pile, 6 m	2.5	0
6	Water pumping station	4	115	Bored pile, 19 m	2.1	10
5	Bank	4	158	Bored pile, 19 m	3.7	20
4	Residential building	4	67	Bored pile, 19 m	3.8	30
3	Residential building	5	110	Prestressed Pipe Pile, 12 m	4.2	40
2	Residential building	5	81	Unknown	6	50
1	Security administration	5	170	Unknown	7.2	70

The seven buildings are all built in the form of a frame structure

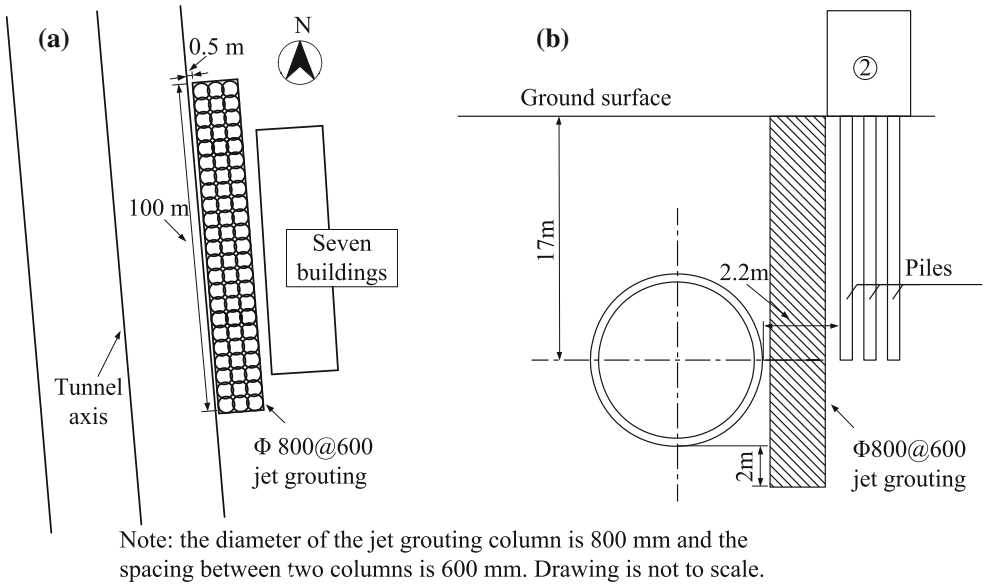

Fig. 2 **a** Plan and **b** sectional view (A–A) of tunnel and building foundations

There are two parallel tunnels. One is excavated towards the north (northbound tunnel) and the other one is excavated towards the north (southbound tunnel) (see Fig. 1c). Their centre-to-centre distance is 15.5 m. The subject in this paper is the southbound tunnel which was excavated first. The centreline of the tunnel was 17 m below the ground surface. Lining rings had an inner and outer diameter of 7.7 and 8.5 m, respectively, and were 0.4 m thick and 1.6 m long.

There were seven buildings at the western side of the tunnel, as shown in Fig. 1c. Table 1 lists the general profile of these buildings. Their distance from the tunnel ranged from 2.1 to 7.2 m. A total of 428 jet-grouted columns were installed between the tunnel and the buildings to prevent large displacement of the buildings and high deformation of the adjacent soil. The total length of the seven buildings was about 80 m, and the jet grouting zone is 100 m, along the direction in which the tunnel was advanced. Figure 2 depicts the layout of the jet-grouted columns. Cement and sodium silicate mixed grout (CSG) was grouted into the ground as the secondary grouting material. Table 2 lists the parameters of the CSG.

The stratigraphy of the site is shown in Fig. 3a. The subsoil profile here consisted of backfill (from 0 to

Table 2 Parameters of cement and sodium silicate mixed grout

Properties	Range
Sodium silicate	39 Be’
Water–sodium ratio by weight	1:1
Water–cement ratio by weight	1:1
Cement grout–sodium solution by volume	3:1
Initial setting time (s)	15–20
Grouting pressure (MPa)	0.3–0.5
Grouting volume per ring (m^3)	2–5

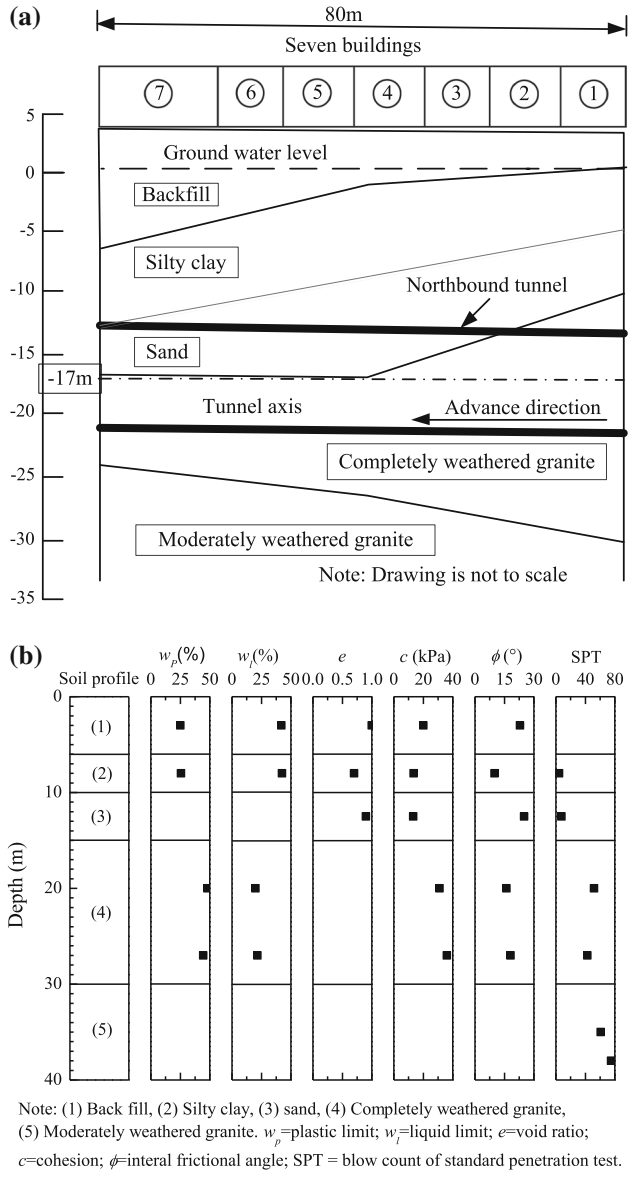

Fig. 3 **a** Cross-sectional view and **b** soil properties of the construction site

10.1 m), quaternary soft deposit (GVI, from 3.4 to 20.8 m), completely weathered granite (GV, from 14 to 34 m), and moderately weathered granite (GIV, from 26.9 m). The excavation face mainly consisted of sand and completely weathered granite. The typical subsurface profiles and soil properties of the test site are depicted in Fig. 3b. The cohesion of these soils ranged from 13.2 to 36 kPa, with internal frictional angle varying between 10° and 25°. A standard penetration test (SPT) is conducted to check the strength of the soil. The mean SPT values of the completely weathered granite and moderately weathered granite ranged from 43 to 52 and from 61 to 75. The groundwater level was 3.5 m below the ground surface.

The weathering classification system is divided into five grades: fresh, slightly weathered, moderately weathered, highly weathered and completely weathered (MOHURD 2014), which is consistent with weathering classification proposed by Ehlen (2002). The structure of completely weathered granite is like hard soil, which collapses easily when pressed by the hands or washed with water. Highly weathered granite is like broken pieces of granite in soil or soil sand. It collapses easily when soaked in water. Moderately weathered granite, which is block-shaped with coarse grain in fragment to massive, has abundant weathered fractures. Slightly weathered granite has few weathered fractures and has high strength, with a high uniaxial compressive strength (UCS) of more than 100 MPa.

The property of granite in Humen is the same to that of granite all over Guangdong Province, including Shenzhen (Cui et al. 2016). The granite was generally formed in the Cretaceous and Jurassic periods. The mineral composition of the granite consists of feldspar and quartz. In southeast China, there are four genetic types of granite, remelting type, syntectic type, differentiation type and metamorphic–metasomatic type. Most of the granites in Humen are the syntectic type, and the rest are the re-melting type. The syntectic granite, which distributed adjacent to the fault zone, is formed by the synthetic effect of intrusive rock and continental crust material. The lithology mainly includes adamellite, granodiorite and biotite granite, and the occurrence is stock or dike.

The granite in Humen, whose tectonic is granular, porphyritic or porphyroid, is medium to coarse grain and exists in massive structures. The granite mainly includes minerals like silica and alkali feldspar. It has mainly been weathered by chemical weathering, which changes the minerals and chemicals present. During the process of weathering, the plagioclase decomposes first, and then the orthoclase and the biotite. The main products of weathering are clay minerals and silica, which have large pores that keep the granite residual soil within the structure of the parent rock.

The EPBM employed in this project was an earth pressure balance (EPB) shield machine with a diameter of 8810 mm to excavate the tunnel in the layers composed of completely to slightly weathered granite, which was the upper-soft lower-hard ground. Figure 4 shows the cutter head of both rippers and disc-cutters of the TBM, which can cut through hard rock having an unconfined compressive strength (UCS) of more than 200 MPa. The strength of the rock environment shown in this manuscript was only up to 50 MPa. However, full-face rock granite with unconfined compressive strength up to 180 MPa has been encountered in some other part of the rock along the tunnel alignment. Therefore, we used the earth pressure balance shield boring machine (EPBM) in this project.

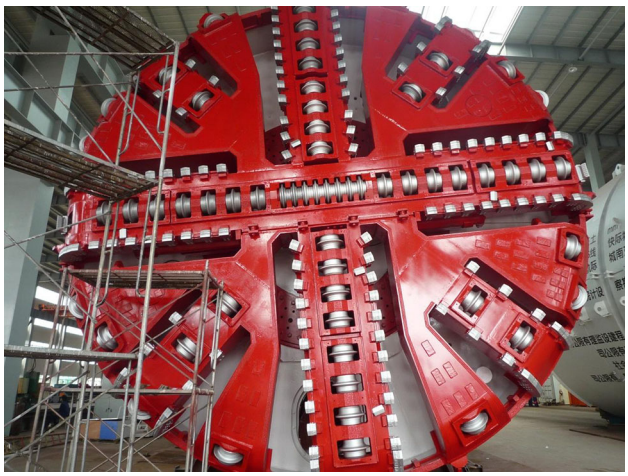

Fig. 4 Cutter head of the TBM

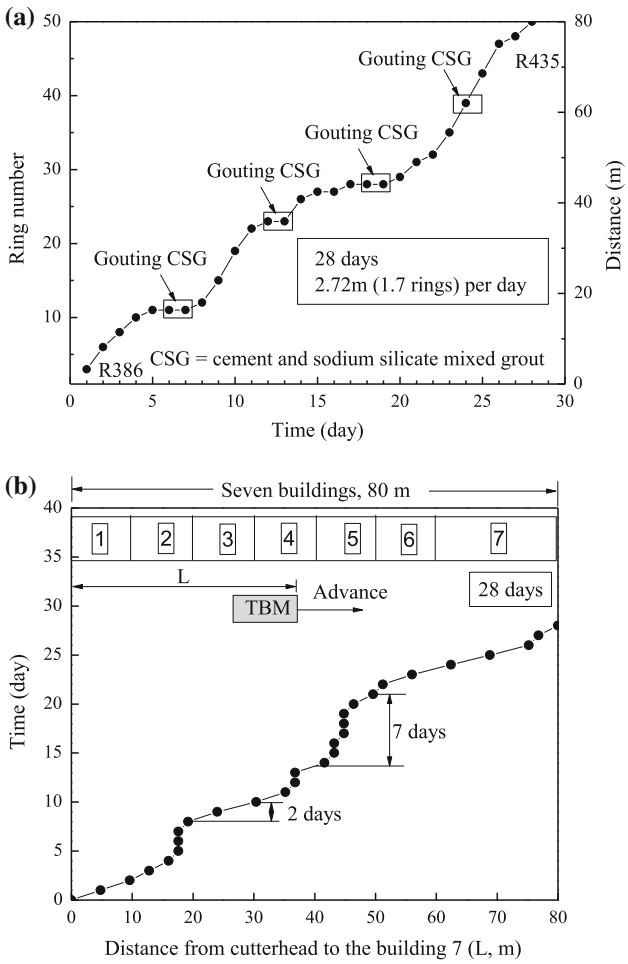

Fig. 5 Tunnelling progress curve of passing below the seven buildings

Figure 5a depicts the tunnelling progress curve. It took 28 days for the EPBM to pass through the seven buildings from R368 to R435. The average advance speed was 2.72 m (1.7 rings) per day. The position of the EPBM cutter head is also shown in Fig. 5b. CSG was grouted four times into the soil. It took almost 7 days to pass through building 3 and 6 days to pass through building 6, which were relatively longer than the other five buildings.

Field test programme

During the tunnelling excavation under the seven buildings, lateral displacements of the subsoil, and horizontal displacements and settlements of the buildings were monitored. The monitoring instruments included one total station, 28 settlement gauges (C1–C28), and four soil inclinometers (I1–I4). Figure 6 shows the layout of the monitoring points. The settlement gauges were installed at the four corners of each building. The horizontal displacements were monitored by the total station. The horizontal displacement measuring points of the buildings were positioned at two corners close to the tunnel. The inclinometers were installed at 25 m depth. The four soil inclinometers (I1–I4) were 2.5, 2.1, 3.7 and 3.8 m away from the tunnel. The test monitoring frequency for the three items was twice a day (12 h interval).

In case of cutter wear during passing under the seven buildings and the risk to replace cutters, when the EPBM was 15 m from the buildings, it was stopped for the examination of the cutter disc, which might be damaged and required replacement in the past tunnelling. Test monitoring started when the EPBM was stopped. It took 12 days to replace the cutters. After this, the EPBM was restarted to continue the excavation, and reached the buildings in 3 days. The total duration for the monitoring of tunnelling excavation effects on the adjacent buildings was 70 days, including monitoring at 15 days before, 28 days during and 21 days after passing under the seven buildings.

Observed results

Vertical displacements of buildings

Figure 7 shows the vertical displacements of the seven buildings induced by the tunnelling excavation. Positive vertical displacements indicate the heave of the building, whereas negative values denote the settlement of the building. The pattern of vertical displacements of one side of each building is very similar. During the 12 days of cutter replacement, it can be observed that 1 mm heave occurred during the first 7 days when the EPBM was stopped, and then almost 2 mm settlement occurred in the following 5 days before the EPBM was restarted (Fig. 7a,

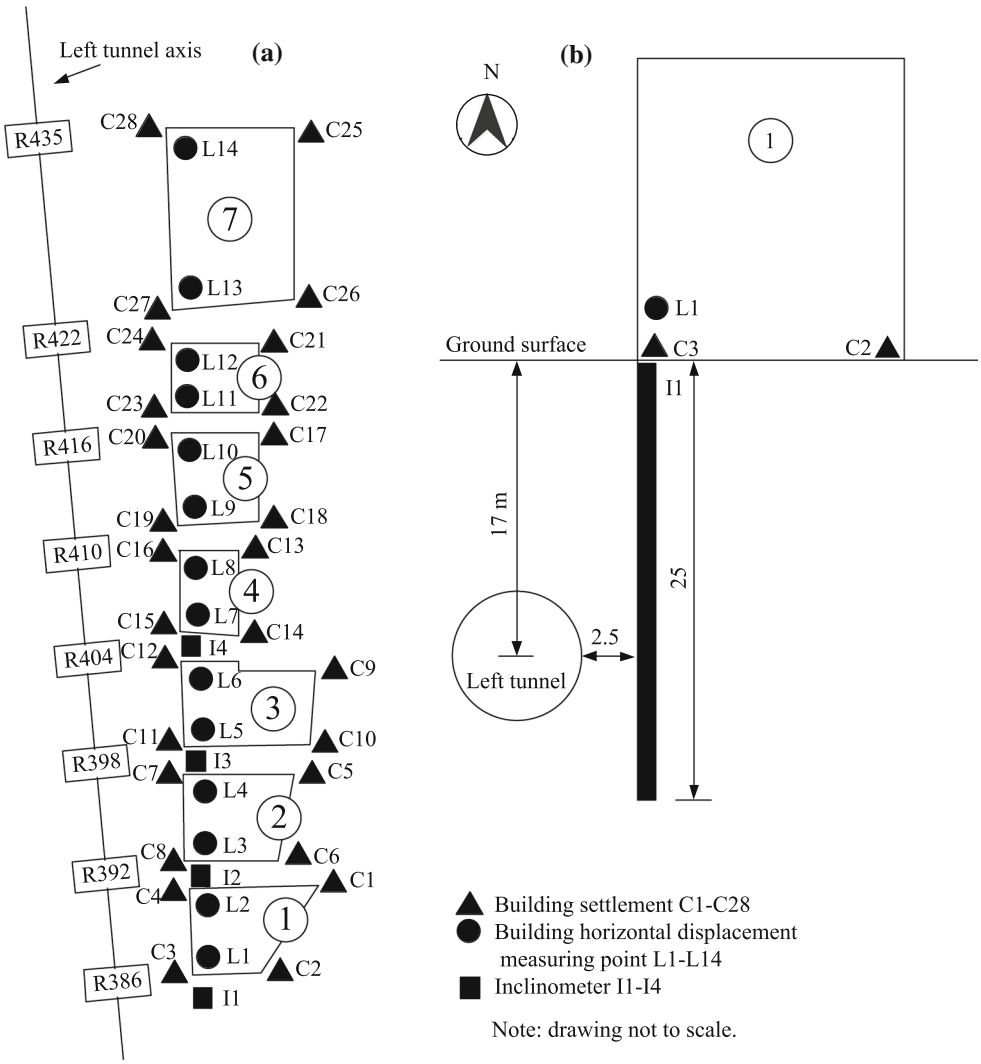

Fig. 6 Field instrumentation: **a** plan and **b** sectional view

b), which indicates that the field monitoring made later is reliable and the error is acceptable, and the former tunnelling excavation had little influence on the test monitoring of the seven buildings.

As shown in Fig. 7a, there is a 2 mm heave before the EPBM arrived at building 1. After the EPBM left building 1, the building settlements increased. But there is a heave of about 1 mm due to the second grouting of CSG after which the building settlements increased. Another obvious cause of heave of 0.5–2 mm was found due to the fourth grouting of CSG (Fig. 5). The settlements of C3 and C4 are larger than those of C1 and C2 because C3 and C4 are closer to the tunnel (Fig. 6). The deviation between them is increasing. The building settlements of C3 and C4 are within 10 mm, which means building 1 was little affected by the tunnelling excavation.

The behaviour of the building settlements of the other six buildings is similar to that of building 1. For each building, the maximum settlements occurred near the tunnel (C3, C4, etc., as shown in Fig. 7). The maximum settlements observed for each building were 9.5 mm (C4), 12.3 mm (C7), 18.9 mm (C10), 17.8 mm (C14), 10.1 mm (C19), 8.7 mm (C22), and 5.7 mm (C26), when the EPBM was 80 m away from building 7. As can be seen, the maximum settlements of C10 (building 3) and C14 (building 4) were higher in comparison with the other five buildings. It can be concluded that before the EPBM head arrived at the building, there was 0–2 mm heave (Phase 1). Then the building settlements began to increase (Phase 2). The building settlements would reduce by 1–3 mm with the CSG grouting.

Horizontal displacements of seven buildings

Figure 8 shows the horizontal displacements caused by the tunnelling excavation. That all the horizontal displacements are positive suggests that the buildings were displaced away from the tunnel. About 1.5 mm horizontal displacement (Fig. 8a, b) was observed during the 12 days

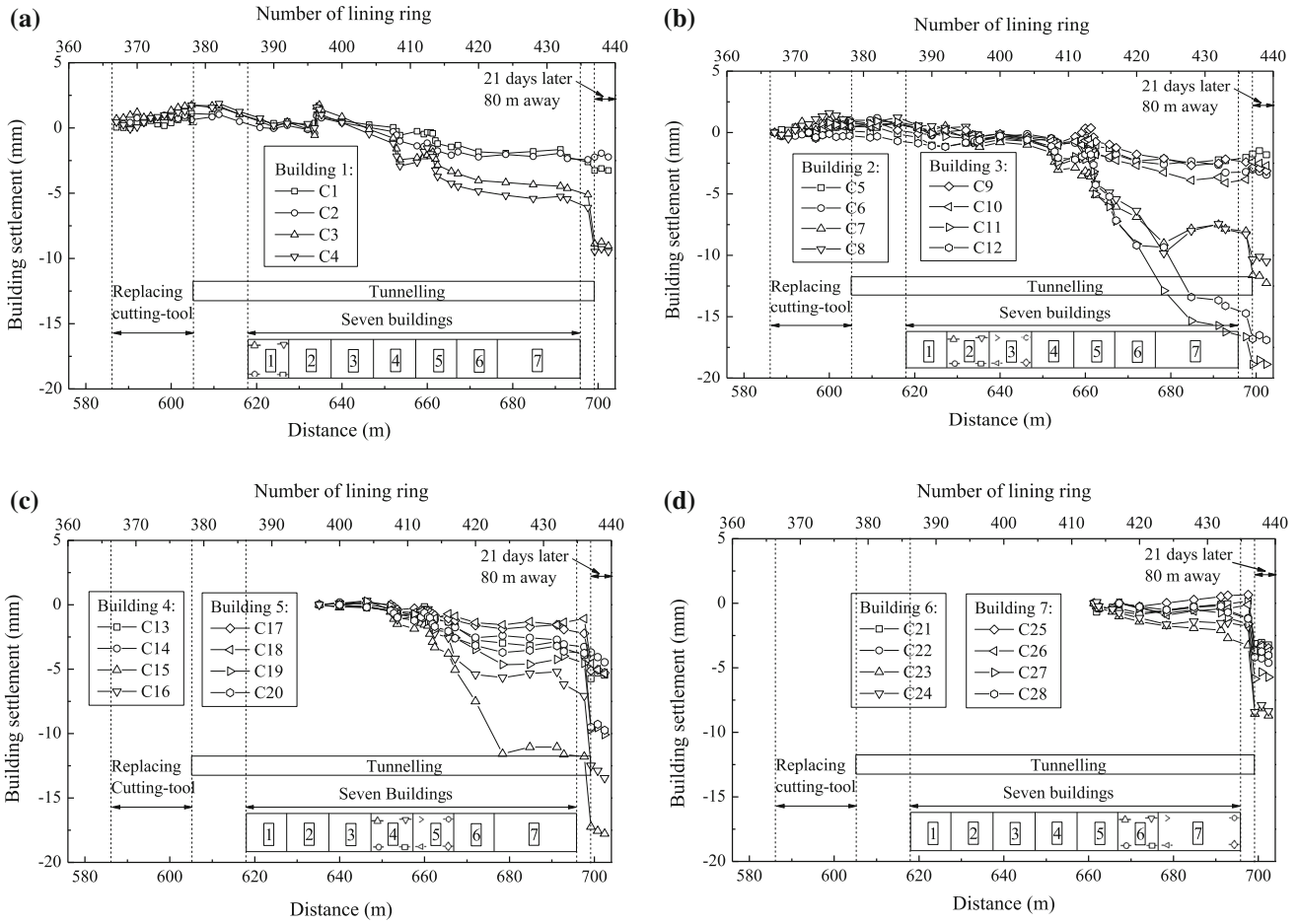

Fig. 7 Settlement of buildings: **a** building 7; **b** building 5 and 6; **c** building 3 and 4; **d** building 1 and 2

of cutter replacement, which suggests that the field monitoring made later is reliable and the error is acceptable, and the former tunnelling excavation barely affected the test monitoring of the seven buildings.

As shown in Fig. 8a, there is a 2 mm horizontal displacement before the EPBM arrived at building 1. But the horizontal displacements did not increase while the EPBM passed building 7. After the EPBM left building 1, the building horizontal displacements increased by 1 mm due to tail skin grouting, and then they continued to increase. However, there is a decline of about 1 mm, possibly due to the unloading of the surrounding soil. Then the building horizontal displacements quickly increased after this due to the second grouting of CSG.

The behaviour of the building settlements of the other six buildings is similar to that of building 1. The horizontal displacements of each building increased with the advance of the EPBM. The maximum horizontal displacements observed were 6.5 mm (L2), 6.9 mm (L3), 8.8 mm (L6), 8.3 mm (C7), 7.8 mm (L9), 7 mm (L12), and 6.1 mm (C13). As can be seen, the maximum horizontal displacements of L6 (building 3) and C7 (building 4) were larger in comparison with the other five buildings.

Lateral ground displacements of ground

Figure 9 shows the lateral displacements caused by the tunnelling excavation as observed by inclinometer I1, I2, I3 and I4 after the EPBM passed the seven buildings 21 days later, which was 80 m away. The pattern of the lateral displacements is very similar. For every inclinometer, the maximum lateral displacements were 6.4 mm (I1), 6.7 mm (I2), 6.4 mm (I3) and 5.6 mm (I4), approximately at the level of the tunnelling zone, with significant mass movements of the ground. The lateral displacements of I3 and I4 were 2 mm larger than those of I1 and I2 up to a depth of 8 m, which is in accordance with the building horizontal displacements.

Analysis on construction procedure

Figure 10 presents the field observed total thrust curve during excavation. The total thrust ranged between 20,000 and 40,000 kN. There was an upward shift of the total thrust around R410 as the stratum was changing into one

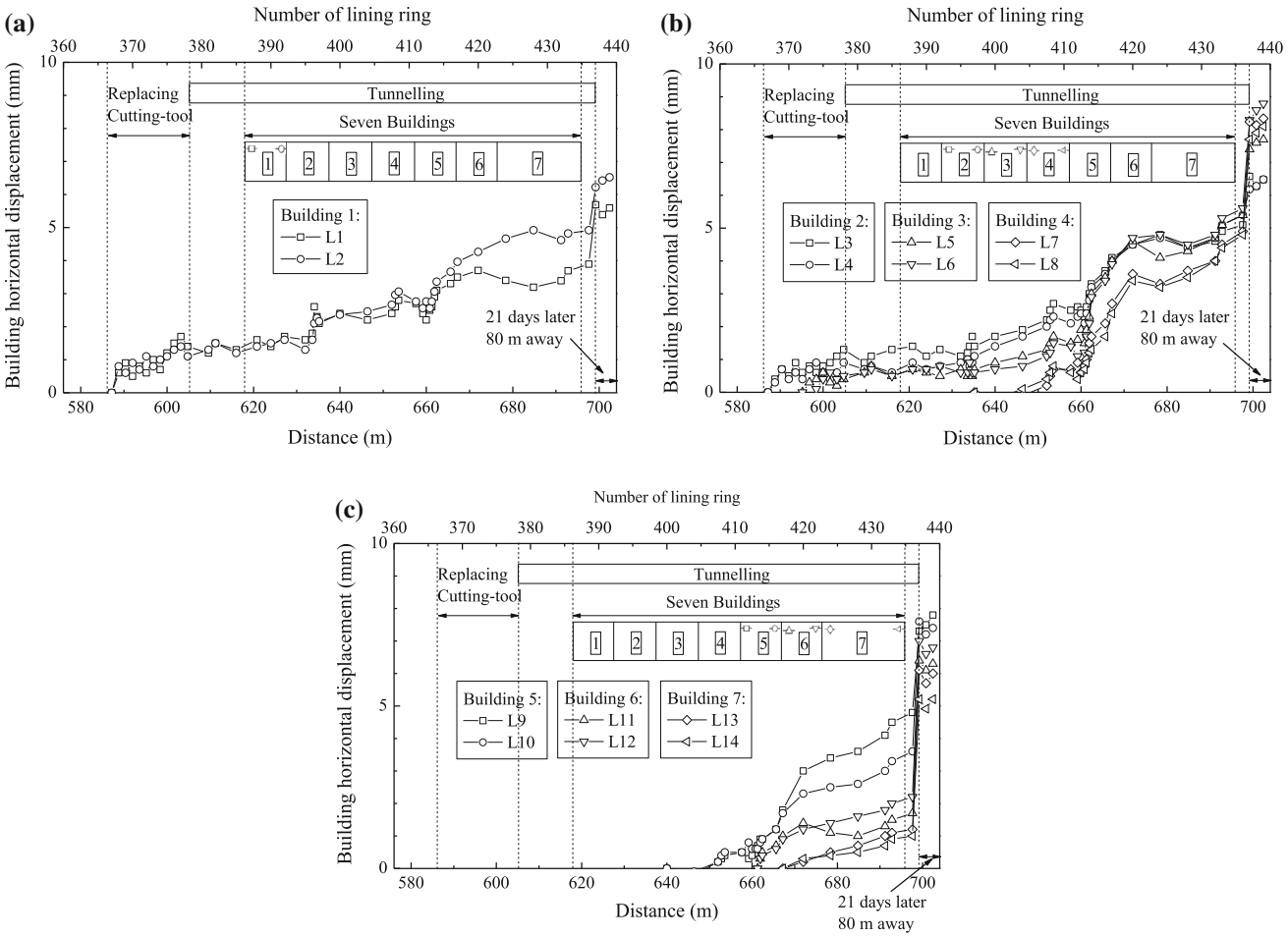

Fig. 8 Horizontal displacements of building: **a** building 7; **b** building 4, 5 and 6; **c** building 1, 2 and Building 3

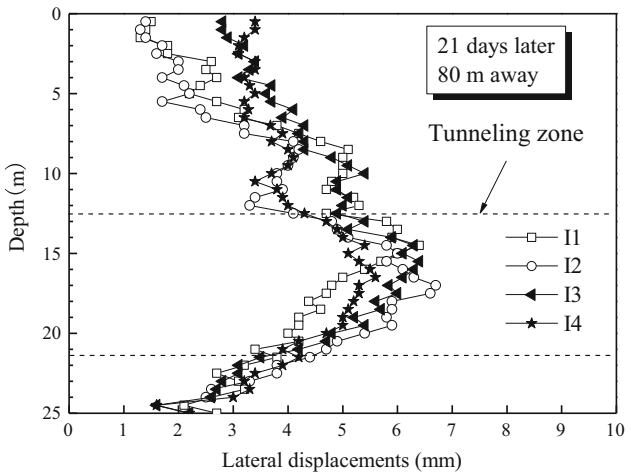

Fig. 9 Lateral displacements of subsoil at inclinometer I1, I2, I3 and I4

with a higher percentage of residual soil, which may have caused larger settlements and horizontal displacements of building 3 and building 4 in comparison with the other buildings. Before and after this stage, the disturbance induced by the tunnelling excavation is relatively small. Actually, the mean total thrusts before and after ring number R410 were 27,000 and 34,000 kN, an increase of 31 %. The reason for the variation of these parameters was the stratum change from completely weathered granite to the composite of residual soil and completely weathered granite (see Fig. 2), which was the upper-soft lower-hard ground. This kind of ground caused many difficulties in the tunnelling such as high cutter wear and flat cutters and tunnel face instability (Zhao et al. 2007). And this is why the EPBM was stopped to examine of the cutter disc when it was 15 m away from the seven buildings.

The soil chamber pressure, affected by the thrust of the EPBM, the rotation rate of the screw, and the opening at the end of the screw, was adjusted to balance the face pressure at the cutter head. As can be seen in Fig. 11, the soil chamber pressure decreased before R410 as the percentage residual soil became higher with the excavation face. And after the R410, the soil chamber pressure increased rapidly and then stabilised as the percentage of

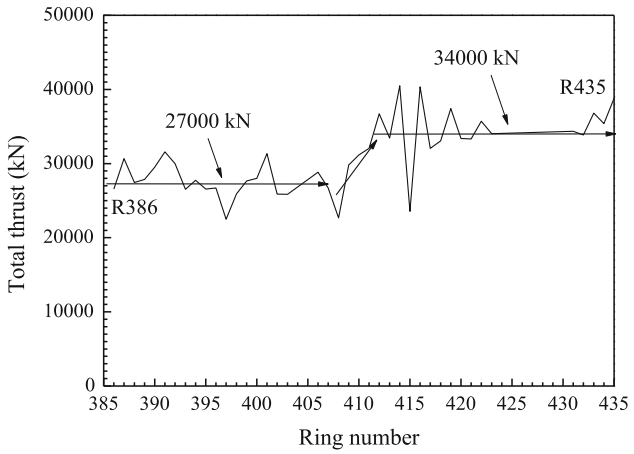

Fig. 10 Variation of total thrust during tunnelling excavation

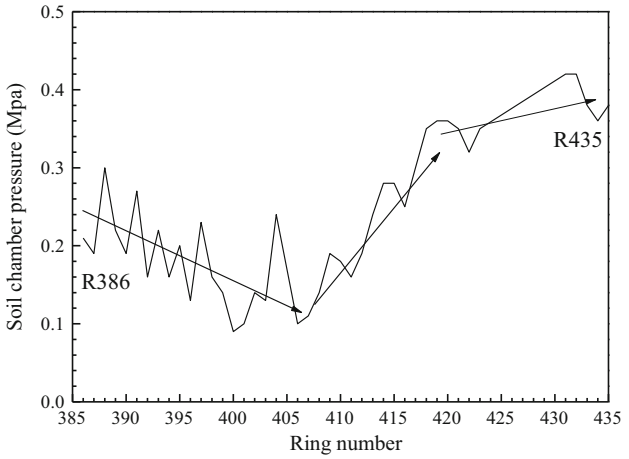

Fig. 11 Variation of soil chamber pressure during tunnelling excavation

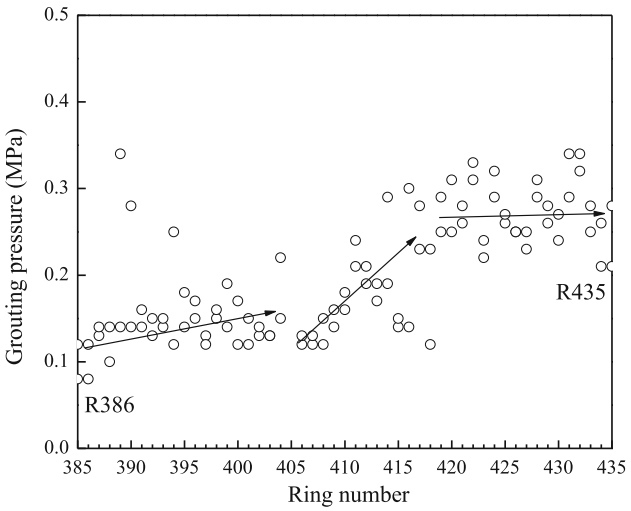

Fig. 12 Variation of grouting pressure during tunnelling excavation

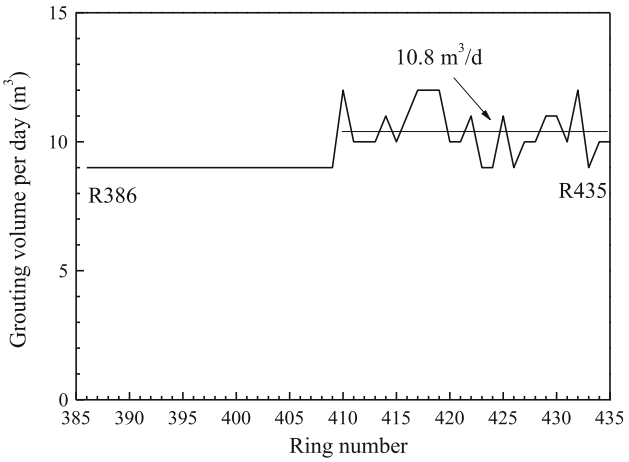

Fig. 13 Variation of grouting volume during tunnelling excavation

residual soil became stabilised. After R410, there were no large displacements of building 5, 6 and 7 which mean the adjustment of the soil chamber pressure is effective.

Figure 12 shows the grouting pressure at the tail-skin grouting which aims at filling the annular void between the ground and the lining. The grouting pressure shows the same tendency as the total thrust curve. The range of the mean grout pressures per ring varies from 0.1 to 0.28 MPa. Figure 13 shows the daily grouting volume. The mean grouting volumes before and after R410 are 9 and 10.8 m^3/day. The larger grouting pressure and grouting volume after R410 are to prevent the building 5, 6 and 7 from large displacements.

As shown in Fig. 5, it took 28 days for the EPBM to pass the seven buildings. The mean excavation speed is 1.7 rings per day. Regarding building 3 and building 5, the mean excavation speeds are 0.95 rings and 3.33 rings per day, respectively. Despite the lower excavation speed of building 3, its displacement is larger than that of building 5. Therefore, it is possible that within a certain range, the excavation speed is not the main factor for the displacements of the building.

Table 3 lists a comparison of the EPBM operation parameters in normal tunnelling excavation and the tunnelling excavation passing through the seven buildings. It can be concluded that a low penetration rate and a low excavation speed should be adopted and the thrust and the soil chamber pressure should be adjusted according to the stratum for the EPBM to safely pass through the seven buildings.

After the analysis of the tunnelling excavation effects on the seven adjacent buildings, requirements of tunnelling excavation passing near buildings in upper-soft lower-hard ground are proposed:

Table 3 TBM operation parameters

Operation parameters	Normal	Below seven buildings
Total thrust (kN)	14,000–32,000	38,000–48,000
Penetration rate (mm/min)	45–70	10–25
Soil chamber pressure (MPa)	0.12–0.32	0.1–0.15
Excavation speed (rings/day)	3–3.5	2

1. Conduct a comprehensive geotechnical exploration of the construction site.
2. Fully overhaul the EPBM ahead of tunnelling construction, especially the cutter head, foam-filled tube, grouting tube, and the tunnel tail sealing, in case of machine faults during the "passing".
3. Install jet-grouting columns or other separation structures between the tunnel and the buildings.
4. Predict and adjust the tail-skin grouting and secondary grouting by adjustment of the grouting material, grouting proportion, grouting pressure and grouting volume.
5. Modify the spoil at the working face if using the EPB method.
6. Monitor the soil deformation and the building displacements and feed back to the construction parameters in time.
7. Adjust the thrust force, excavation speed, screw conveyor mass per ring, penetration speed and posture of the EPBM.

Conclusions

Field monitoring has been conducted to investigate hazards on surrounding facilities within a very close distance of a shield tunnelling machine passing under them. The results of this field investigation are summarised as follows:

1. The hazards on seven buildings during shield tunnelling were within the controllable range. The maximum building settlement was 18.9 mm and the maximum building lateral displacement was 8.8 mm. The maximum lateral ground displacement was 6.7 mm. All of these displacements were within the allowable range of 20 mm for hazards prevention. The construction parameters optimised according to the gradually changing strata through the seven buildings rather than adopted in normal tunnelling could effectively reduce the hazards of surrounding environment during tunnel construction.
2. Different vertical and horizontal displacements have been observed for the seven buildings. The reason was attributed to the different tunnelling operation parameters that varied with the ground stratum. When tunnelling in the upper-soft lower-hard ground as the stratum was changing into one with a higher percentage of residual soil, there was an upward shift of total thrust as well as the soil chamber pressure and grouting pressure, leading to larger settlements and horizontal displacements of the nearby buildings. Within a certain range from 1 to 3.5 rings per day, excavation speed is not the main factor for the displacements of the building.
3. Tail grouting cannot mitigate excessive settlements of the surrounding soil and the adjacent buildings. However, secondary grouting can sometimes restrain the displacements of buildings, but can increase the buildings' horizontal displacements.
4. Requirements to mitigate hazards of environments during tunnelling excavation passing below buildings in upper-soft lower-hard ground are proposed based on this case. This successful case provides an example for future environmental protection construction of shield tunnel in similar geological strata.

Acknowledgments The research work described herein was funded by the National Nature Science Foundation of China (NSFC) (Grant No. 41372283) and National Basic Research Program of China (973 Program: 2015CB057806). These financial supports are gratefully acknowledged.

References

Addenbrooke TI, Potts DM (2001) Twin tunnel interaction: surface and subsurface effects. Int J Geomech 1(2):249–271

British Standards Institute (BSI) (1981) Code of practice for site investigation. British Standard 5930, London Section 44

Blindheim OT, Grøv E, Nilsen B (2002) The effect of mixed face conditions (MFC) on hard rock TBM performance. In: ITA World Tunnel Congress, Sydney, pp 400–407

Cui QL, Shen SL, Xu YS, Wu HN, Yin ZY (2015a) Mitigation of geohazards during deep excavation in karst region with caverns: a case study. Eng Geol 195:16–27

Cui QL, Wu HN, Shen SL, Xu YS, Ye GL (2015b) Chinese Karst geology and measures to prevent geohazards during shield tunnelling in Karst regions with caves. Nat Hazards 77:129–152

Cui QL, Wu HN, Shen SL, Xu YS (2016) Geological difficulties of socket diaphragm walls in weathered granite in Shenzhen, China. Bull Eng Geol Environ 75:263–273

Dearman WR (1974) Weathering classification in the characterisation of rock for engineering purposes in British practice. Bull Eng Geol Environ 9:33–42

Dearman WR, Baynes FJ, Irfan TY (1978) Engineering grading of weathered granite. Eng Geol 12:345–374

Delisio A, Zhao J, Einstein HH (2013) Analysis and prediction of TBM performance in blocky rock conditions at the Lötschberg Base Tunnel. Tunn Undergr Space Technol 33:131–142

Du YJ, Jiang NJ, Shen SL, Jin F (2012) Experimental investigation of influence of acid rain on leaching and hydraulic characteristics of cement-based solidified/stabilized lead contaminated clay. J Hazard Mater 225–226:195–201

Du YJ, Jiang NJ, Liu SY, Jin F, Singh DN, Pulppara A (2014) Engineering properties and microstructural characteristics of cement solidified zinc-contaminated kaolin clay. Can Geotech J 51:289–302

Ehlen J (2002) Some effects of weathering on joints in granitic rocks. Catena 49:91–109

Fargnoli V, Boldini D, Amorosi A (2013) TBM tunnelling-induced settlements in coarse-grained soils: the case of the new Milan underground line 5. Tunn Undergr Space Technol 38:336–347

Hassanpour J, Rostami J, Khamehchiyan M, Bruland A, Tavakoli HR (2009) TBM performance analysis in pyroclastic rocks: a case history of Karaj water conveyance tunnel. Rock Mech Rock Eng 43(4):1–19

Liao SM, Liu JH, Wang RL, Li ZM (2009) Shield tunneling and environment protection in Shanghai soft ground. Tunn Undergr Space Technol 24(4):454–465

Ma L, Xu YS, Shen SL, Sun WJ (2014) Evaluation of the hydraulic conductivity of aquifer with piles. Hydrogeol J 22(2):371–382

Ministry of Housing and Urban-Rural Development of the People's Republic of China (MOHURD) (2014) Standard for engineering classification of rock masses (GB/T 50218-2014), China Planning Press

Norbury D, Hencher S, Cripps J, Lumsden A (1995) The description and classification of weathered rocks for engineering purposes. Geological Society Engineering Group Working Party report. Q J Eng Geol 28:207–242

Shen SL, Han J, Huang XC, Du SJ (2003) Laboratory studies on property changes in surrounding clays due to installation of deep mixing columns. Mar Georesour Geotechnol 21(1):15–35

Shen SL, Xu YS, Hong ZS (2006) Estimation of land subsidence based on groundwater flow model. Mar Georesour Geotechnol 24(2):149–167

Shen SL, Horpibulsuk S, Liao SM, Peng FL (2009) Analysis of the behavior of DOT tunnel lining caused by rolling correction operation. Tunn Undergr Space Technol 24(1):84–90

Shen SL, Du YJ, Luo CY (2010) Evaluation of the effect of double-o-tunnel rolling-correction via apply one-side block loading. Can Geotech J 47(10):1060–1070

Shen SL, Wang ZF, Yang J, Ho EC (2013a) Generalized approach for prediction of jet grout column diameter. J Geotech Geoenviron Eng ASCE 139(12):2060–2069

Shen SL, Ma L, Xu YS, Yin ZY (2013b) Interpretation of increased deformation rate in aquifer IV due to groundwater pumping in Shanghai. Can Geotech J 50(11):1129–1142

Shen SL, Wu HN, Cui YJ, Yin ZY (2014) Long-term settlement behavior of the metro tunnel in Shanghai. Tunnel Undergr Space Technol 40:309–323

Shen SL, Wang JP, Wu HN, Xu YS, Ye GL, Yin ZY (2015a) Evaluation of hydraulic conductivity for both marine and deltaic deposit based on piezocone test. Ocean Eng 110:174−182

Shen SL, Wu YX, Xu YS, Hino T, Wu HN (2015b) Evaluation of hydraulic parameter based on groundwater pumping test of multi-aquifer system of Tianjin. Comput Geotech 68:196–207

Shirlaw JN, Hencher SR, Zhao J (2000) Design and construction issues for excavation and tunnelling in some tropically weathered rocks and soils. In: GeoEng2000 – An International Conference on Geotechnical & Geological Engineering, Melbourne, Australia, pp 1286–1329

Shin HS, Kim CY, Kim KY, Bae GJ, Hong SW (2006) A new strategy for monitoring of adjacent structures to tunnel construction in urban area. Tunn Undergr Space Technol 21:461–462

Tan Y, Wang DL (2013a) Characteristics of a large-scale deep foundation pit excavated by central-island technique in Shanghai soft clay. I: bottom–up construction of the central cylindrical shaft. J Geotech Geoenviron Eng ASCE 139(11):1875–1893

Tan Y, Wang DL (2013b) Characteristics of a large-scale deep foundation pit excavated by central-island technique in Shanghai soft clay. II: top–down construction of the peripheral rectangular pit. J Geotech Geoenviron Eng ASCE 139(11):1894–1910

Tóth Á, Gong Q, Zhao J (2013) Case studies of TBM tunnelling performance in rock–soil interface mixed ground. Tunn Undergr Space Technol 38:140–150

Wang ZF, Shen SL, Ho CE, Kim YH (2013) Investigation of field installation effects of horizontal Twin-Jet grouting in Shanghai soft soil deposits. Can Geotech J 50(3):288–297

Wu HN, Huang RQ, Sun WJ, Shen SL, Xu YS, Liu YB, Du SJ (2014) Leaking behaviour of shield tunnels under the Huangpu River of Shanghai with induced hazards. Nat Hazards 70(2):1115–1132

Wu HN, Shen SL, Liao SM, Yin ZY (2015a) Longitudinal structural modelling of shield tunnels considering shearing dislocation between segmental rings. Tunn Undergr Space Technol 50:317–323

Wu YX, Shen SL, Wu HN, Xu YS, Yin ZY, Sun WJ (2015b) Environmental protection using dewatering technology in a deep confined aquifer beneath a shallow aquifer. Eng Geol 196:59–70

Wu YX, Shen SL, Xu YS, Yin ZY (2015c) Characteristics of groundwater seepage with cutoff wall in gravel aquifer. I: Field observations. Can Geotech J 52:1526–1538

Wu YX, Shen SL, Xu YS, Yin ZY (2015d) Characteristics of groundwater seepage with cutoff wall in gravel aquifer. II: numerical analysis. Can Geotech J 52:1539–1549

Xu YS, Ma L, Du YJ, Shen SL (2012a) Analysis on urbanization induced land subsidence in Shanghai. Nat Hazards 63(2): 1255–1267

Xu YS, Ma L, Shen SL, Sun WJ (2012b) Evaluation of land subsidence by considering underground structures penetrated into aquifers in Shanghai. Hydrogeol J 20(8):1623–1634

Xu YS, Huang RQ, Han J, Shen SL (2013a) Evaluation of allowable withdrawn volume of groundwater based on observed data. Nat Hazards 67(4):513–522

Xu YS, Shen SL, Du YJ, Chai JC, Horpibulsuk S (2013b) Modelling the cutoff behavior of underground structure in multi-aquifer-aquitard ground water system. Nat Hazards 66(2):731–748

Xu YS, Shen SL, Ma L, Sun WJ, Yin ZY (2014) Evaluation of the blocking effect of retaining walls on groundwater seepage in aquifers with different insertion depths. Eng Geol 183:254–264

Xu YS, Yuan Y, Shen SL, Yin ZY, Wu HN, Ma L (2015) Numerical investigation of the land subsidence due to groundwater pumping in Changzhou. Nat Hazards 78:281–296

Zhao J, Broms BB, Zhou Y, Choa V (1994) A study of the weathering of the Bukit Timah granite. Part B: field and laboratory investigation. Bull Int Assoc Eng Geol 50:105–111

Zhao J, Gong QM, Eisensten Z (2007) Tunnelling through a frequently changing and mixed ground: a case history in Singapore. Tunn Undergr Space Technol 22(4):388–400